Original Research Article

Dementia and Geriatric Cognitive Disorders

Dement Geriatr Cogn Disord 2004;17:207–214
DOI: 10.1159/000076358

Accepted: August 13, 2003
Published online: January 20, 2004

Regional Cerebral Blood Flow in Alzheimer's Disease: Classification and Analysis of Heterogeneity

Siegbert Warkentin[a,b] Mattias Ohlsson[c] Per Wollmer[a] Lars Edenbrandt[a] Lennart Minthon[b]

Departments of [a]Clinical Physiology and [b]Psychiatry, Malmö University Hospital, Lund University, Malmö, and [c]Department of Theoretical Physics, Lund University, Lund, Sweden

Key Words

Alzheimer's disease · Artificial neural networks · Cerebral blood flow · Heterogeneity, regional cerebral blood flow

Abstract

Neural networks have been successfully applied to brain perfusion images to classify patients with Alzheimer's disease from normal or other patient populations. Given the recognition that Alzheimer's disease constitutes a heterogeneous disorder, the identification of subgroups sharing common functional brain deficits would constitute a further improvement in the utility of such methods. Therefore, we aimed to investigate whether neural networks could discriminate cortical perfusion deficits of patients with Alzheimer's disease from normal brain perfusion. A second step was to identify subgroups of patients sharing similar perfusion deficits. The study population consisted of one group of 92 normal healthy subjects and one group of 132 patients with mild-to-moderate Alzheimer's disease. The patients were diagnosed according to established criteria (DSM-IV and NINCDS-ADRDA). Regional cerebral blood flow was assessed by the non-invasive ^{133}Xe inhalation method, using a 64-detector system for measurements of blood flow in superficial cortical areas. The regional blood flow values were used as the only input to artificial neural networks with multilayer Perceptron architecture. The networks were trained using the back-propagation updating algorithm. A fourfold cross validation procedure was used in order to obtain the most reliable performance of the networks. The performance of the neural network, measured as the area under the receiver-operating characteristic curve, was 0.94, with a sensitivity for Alzheimer's disease of 86% at a specificity of 90%. An analysis of the relative importance of cortical areas in the discrimination showed that left parietal areas were more important than the right homologous ones. A clustering analysis of the Alzheimer patients identified three or four subgroups of patients with clearly different combinations of blood flow pathology. A consistent finding in all subgroups was a significant deficit in temporoparietal blood flow of both hemispheres. Distinct group differences were seen in frontal, central and occipital areas with different combinations of involvement. This is the first study in which neural networks have been applied to brain perfusion images obtained with the ^{133}Xe inhalation method. The results demonstrate that a classification of patients with Alzheimer's disease obtained with this method is compatible with the best results obtained with other brain imaging methods. The identification of clearly distinguishable patterns of blood flow pathology in subgroups of patients lends further support to the notion that Alzheimer's disease is a heterogeneous disorder.

KARGER

Fax + 41 61 306 12 34
E-Mail karger@karger.ch
www.karger.com

1420–8008/04/0173–0207$21.00/0

Accessible online at:
www.karger.com/dem

Siegbert Warkentin, PhD
Department of Clinical Physiology
Malmö University Hospital
SE–205 02 Malmö (Sweden)
Tel. +46 40 33 14 09, Fax +46 40 33 78 75, E-Mail siegbert.warkentin@skane.se

Introduction

Alzheimer's disease (AD) is the most common cause of severe intellectual decline in dementia and represents a growing burden to societies with an increasing elderly population. The disease is an age-related condition affecting about 10% of the population over 65 years of age and about 50% over age 85 [1] and is characterized by a slowly progressive memory failure, visuospatial disorientation, dysphasia, dyspraxia and dysgnosia. The definite diagnosis of AD can only be obtained from a neuropathological examination, and the hallmarks of the disease include β-amyloid plaques, dystrophic neurites associated with plaques, and neurofibrillary tangles within nerve cell bodies. The topographic distribution of AD pathology has been described to progress in a stereotypical fashion in which medial temporolimbic areas are affected first, followed by neocortical association areas [2].

Together with the psychiatric assessment of symptoms, measurements of regional cerebral blood flow (rCBF) have been used for many years as a clinical tool to describe the functional deficits in the brain of patients with AD [3, 4]. Several comparisons between the rCBF pathology and postmortem neuropathological diagnosis have shown an excellent agreement in cases of AD assessed by the two-dimensional ^{133}Xe inhalation method [5, 6]. Similar sensitivity/specificity rates have been reported in comparisons of autopsy-confirmed cases of AD and temporoparietal perfusion deficits assessed by single photon emission computed tomography (SPECT), or in combination with a measure for medial temporal lobe atrophy by CT [7].

A differential diagnosis of AD is sometimes difficult, especially in the early phase of the disease when symptoms are sparse or when only mild cognitive changes may be seen. In this case, the clinician's experience with the method decides whether the functional brain imaging findings are to be judged as normal variation or whether they might represent early aberrations of clinical importance. Such subjective evaluations are prone to substantial individual variations between clinicians and may lead to a large variability in the diagnostic interpretation, even among well-trained physicians [8]. In order to objectify the process of image interpretation, artificial neural networks have been used as an aid to classify abnormal perfusion and brain metabolic patterns in AD [9–15]. Such studies have usually shown to yield a moderate-to-high discriminatory power between groups of non-demented and demented patients, with a sensitivity ranging from 43 to 100% and specificity rates ranging from 60 to 100% [16]. Although decreased temporal and parietal blood flow and metabolism are usually described as the most discriminating areas between patients and controls [17], the existence of a substantial individual variability in cerebral blood flow deficits has also been recognized in several studies. For example, Holman et al. [18] reported normal SPECT perfusion patterns in 7.7% of AD cases, whereas temporoparietal abnormalities were seen in 26.9% and frontal defects in 5.8% of the cases. A heterogeneity in perfusion patterns was also reported in a SPECT study by Waldemar et al. [19], where temporal or parietal rCBF deficits were seen in 81–86% of AD patients, whereas additional frontal rCBF deficits were seen in 35–76% of patients. Zimmer et al. [20] analyzed individual patient blood flow obtained with SPECT in 92 probable AD patients. They reported a large variability in perfusion deficits among patients, and found that temporoparietal deficits were as common as deficits in temporofrontal perfusion areas.

The objectives of the present study were (1) to investigate whether artificial neural networks could be used to classify data obtained from two-dimensional cerebral perfusion images of AD patients and from normal controls, and (2) to perform a systematic analysis of the heterogeneity of cortical functional pathology patterns in AD.

Patients and Methods

Normal Subjects

Ninety-two normal healthy subjects were recruited through local advertising and gave their written consent to participate in the study. Subjects were mainly hospital employees and university students. Their mean age was 39.1 years (range: 18–72 years), 56 males and 36 females. All subjects underwent a somatic and mental workup including routine laboratory investigation, physical examination and psychiatric screening, in order to exclude somatic illness, histories of psychiatric illness, neurological disorder, abuse of alcohol or drugs, and head injury.

Patient Population

One hundred and thirty-two patients with possible or probable AD were included. Demographic characteristics are shown in table 1. The patients who entered the study were consecutive patients admitted for clinical evaluation of dementia at the Neuropsychiatric Clinic, Malmö University Hospital, Malmö, Sweden. All patients underwent a thorough clinical investigation, including medical history, psychiatric assessment, physical and neurological examination, screening laboratory blood tests, analysis of cerebrospinal fluid, computed tomography, and measurements of rCBF. No patients were treated with cholinesterase inhibitors at the time of investigation.

The diagnosis of AD was made by exclusion of other dementias, in accordance with the National Institute of Neurological and Communication Disorders and Stroke-Alzheimer's Disease and Related Disorders Association (NINCDS-ADRDA) criteria [21]. The degree

of cognitive impairment was evaluated by the Minimental State Examination (MMSE) [22].

The study was approved by the Research Ethics Committee at Lund University and by the Radiation Safety Committee at Malmö University Hospital. All patients and normal control subjects gave their informed consent to participate in the study, in accordance with the provisions of the Declaration of Helsinki.

Cerebral Blood Flow Imaging

The rCBF was measured by the non-invasive ^{133}Xe inhalation method as described by Obrist et al. [23] and Risberg [4]. This method gives information about the blood flow in superficial cortical areas only. Thus, blood flow in deeper structures (such as white matter or basal ganglia) cannot be obtained with this method. In the present study we used a system with 64 scintillation detectors [NaI (Tl) crystals, ¾ × ¾″] arranged in a helmet around the head (Cortexplorer 64, Ceretronix, Randers, Denmark). The system adjusts for differences in head size and shapes, and the positioning of the head is standardized in relation to bony landmarks (nasion and ear channels) by means of light crosses. This makes it possible to reposition subjects accurately in case of head movements.

The measurement procedure was as follows: After a 30-second measurement of the natural background radiation, a mixture of the inert γ-emitting tracer ^{133}Xe (90 MBq/l) and air was inhaled by the subject for 1 min through a facemask. During the following period of 10 min, the subject breathed normal air, according to the standard procedure [23]. Thus, the total duration of one rCBF measurement was 11.5 min. The data obtained with the present method represent an average of flow during the washout period. The tracer diffuses into brain tissue from arterial blood and is cleared by venous blood. Blood flow values were calculated from the rate of clearance of the isotope considering also the changes of the arterial concentrations of ^{133}Xe, the latter estimated from the isotope concentration in the end-tidal air, sampled from the facemask. The lowest acceptable peak count rates were 1,500 counts/second. The initial slope index (ISI, 2–3 min slope measurement) was used, because this flow parameter has shown to have a high stability and reliability also in pathological conditions [24]. The arterial partial pressure for CO_2 was estimated from the end-tidal CO_2 concentrations (Ohmeda gas analyzer), $P_E \cdot CO_2$. Measurements of respiration, blood pressure and heart rate were performed continuously during the rCBF recordings.

Flow values for each detector were calculated as distribution normalized values, based on the hemispheric mean values. The values were used in the neural network analyses. A color graphics system (Cortexplorer 64) was used for the presentation of the flow maps. The algorithm for calculation of a given pixel in the maps was based on a weighted linear interpolation of the distance to the four closest detectors. In this way interpolated color-coded maps were created, which show the distribution normalized values. The illustrations shown in figures 3 and 4 represent pixel-by-pixel statistical comparisons between normal subjects and patients (Student's t test).

Artificial Neural Networks

Feed-forward artificial neural networks with a standard multilayer Perceptron architecture were used. A general introduction to the subject can be found elsewhere [25]. The neural networks consisted of one input layer, one hidden layer and one output layer. The inputs to the neural network were the ISI 2–3 distribution normalized values from the detectors on which the rCBF images were based. Four detectors (two prefrontal and two occipital) were not used because they were found to be prone to artifacts (fig. 2). The output layer consisted of one node that encoded whether the image was normal or consistent with AD. A Kullback-Liebler error function was used together with a Langevin extension [26] of the back-propagation updating rule. Langevin updating consists of adding a random number Gaussian component to the weight updates, which has the effect of speeding up the minimization procedure.

In order to assess the generalization performance, the full rCBF data set was divided into four equally sized parts. Each of these parts was used as a test set and the remaining three parts were used as training sets in a 4-fold cross validation scheme. In order to avoid overtraining, a weight elimination regularization term was used [27]. For each test set, a committee of 30 networks was trained on the corresponding training set and the output from a committee was calculated as the mean across its 30 members. The output values for the test rCBF values were in the range from 0 to 1. A threshold in this interval above which all values were regarded as consistent with AD was used to calculate the sensitivity and specificity. By varying this threshold a receiver-operating characteristic (ROC) curve was obtained. The area under the ROC curve represented the neural networks performance. The 95% significance level of the ROC area was calculated using the bootstrap method [28].

Sensitivity Analysis

A sensitivity analysis was performed that, qualitatively, measured the importance of the different neural network inputs, i.e. the different detectors. The following procedure was used: The training error for the final committee of networks was computed. For each of the detectors, a new training error was calculated by removing that detector, i.e. replacing it by its mean value across the population. The increase in training error when removing a detector was used as a measure of its importance. The analysis resulted in a list with a value of importance for each detector. From this list, the most important detectors, i.e. those which after removal from the data set gave the highest increase in the training error, were identified. The mean of the importance measure for the left and for the right detectors were calculated. The significance of this left-right difference was calculated using a permutation test [28] according to the following procedure: The importance measures were arranged as two lists, one for the left hemisphere detectors and one for the right hemisphere detectors. The test was then performed by repeatedly and randomly permutating the importance measures in the two lists. For each permutation, the difference in the means of the two resulting lists were calculated (test statistic). The evidence against the null hypothesis of no difference between the two original means was given by the fraction of area differences of the test statistic larger than the actual difference. This resulted in a significant difference between the hemisphere detectors ($p < 0.013$), showing that the left hemisphere detectors were more important for the discrimination of AD than the right hemisphere detectors.

Clustering Analysis

A clustering analysis was performed which divided the patients consistent with AD into three or four different groups. The division was carried out using the K-means clustering algorithm [29] and where the rCBF detector values were the only source of information. Several clusterings were performed and the Davis-Boulder index [30] was used in order to select good clusterings. The clustering procedure was performed such that each of the 132 AD patients was represented by a 60-dimensional vector, consisting of the rCBF values

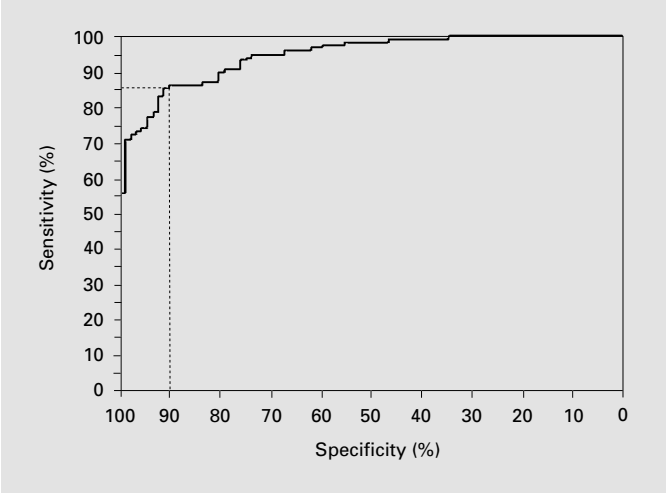

Fig. 1. The ROC curve for the classification of rCBF images into normal or consistent with AD. The area under the ROC curve is 94.7% (92.7, 97.0%). The values in parentheses are the 95% confidence levels, obtained by a bootstrap method.

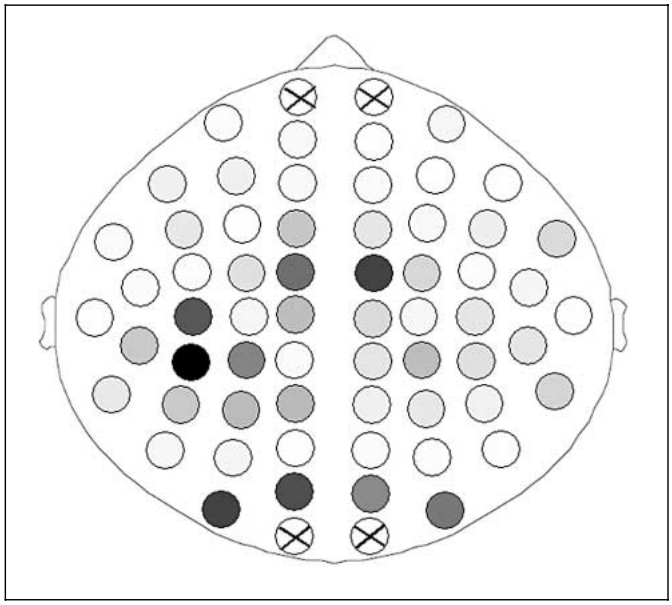

Fig. 2. The location of the detectors from a vertex view. Frontal areas are shown at the top, and the left hemisphere is on the left side. The illustration shows the most important detectors discriminating normal subject values from those with AD. The level of grey indicates the size of the importance measure; the more grey the more important. The four detectors marked by crosses where not part of the analysis, since they were prone to artifacts.

from the detectors. The objective was to find clusters in this 60-dimensional space using the K-means clustering algorithm [29]. However, this is a non-trivial task because of relatively few data points in a high-dimensional space. Two independent clusterings using the K-means algorithm may, therefore, not result in the same division. To overcome this problem, a more statistical viewpoint was taken, where many independent clusterings were performed, and good ones were selected based on the Davies-Bouldin index. This index measures the ratio of the intra- and inter-cluster distances, favoring clusterings with compact and well-separated clusters. The index is independent of the number of clusters used, and it was found that three or four clusters resulted in the lowest indices.

For the results presented in this paper, 5,000 independent clusters were performed, for both K = 3 and K = 4, and the 5% with the best indices were kept. These were further analyzed to select clusterings with stable clustering positions. Finally, each cluster was marked AD group 1, AD group 2, for example, and an AD patient was said to belong to a given group if the majority of the selected clusterings was consistent with that group.

Results

The normal control group was significantly younger than the patients ($p < 0.0001$, Student's t test). It is well known that age is significantly correlated with the general perfusion level of the cortex in normal subjects [31]. Age-related changes in rCBF are on the other hand small in magnitude and affect primarily frontal areas and to a negligible degree postcentral areas [32]. Therefore, we chose only regional flow values as input to the neural networks, to minimize the effect of age as a confounding factor.

The performance of the neural network is shown in figure 1. The area under the ROC curve was 94.7%, with a 95% confidence interval of 92.7 and 97.0%, respectively. The sensitivity for AD was 86% at a specificity of 90%.

Figure 2 shows the regional areas important for the neural network classification. As can be seen by the importance measure (level of shaded grey), left parietal areas were more important in the classification than right parietal areas, which was significant ($p < 0.013$). The regional flow pattern of the normal control group (fig. 3) showed the well-known so-called 'hyperfrontal' distribution, with higher relative values in frontal and frontotemporal areas, compared to other areas [4, 33]. When the rCBF pattern was compared with the normal pattern, AD patients showed the 'typical' temporoparietal flow pathology, with significantly higher distribution values in motor areas and in occipital areas.

RCBF Clusters of Alzheimer's Disease

Table 1 shows the demographic characteristics and the cerebral perfusion values of the patients. There was no

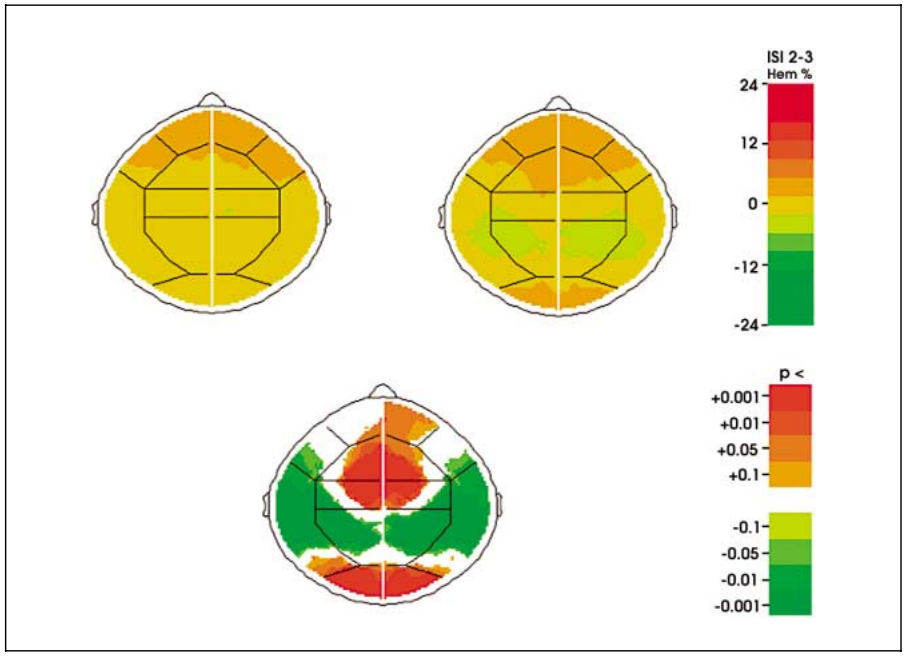

Fig. 3. Upper left: vertex projection of the cortical blood flow distribution (percent of the hemispheric mean) of normal controls (n = 92). Distribution values are color coded according to the bar to the far right. Orange to red = Higher values than the hemispheric mean; yellow = equal to the hemispheric mean; green = lower than the hemispheric mean. Upper right: vertex projection of cortical blood flow distribution in Alzheimer patients (n = 132). Lower: statistical comparison (Student's t test) between Alzheimer patients and normal controls. Statistical significance levels are coded according to the bar to the far right. Red = Significantly higher values in patients compared to normal controls; green = significantly lower in patients compared to normal controls.

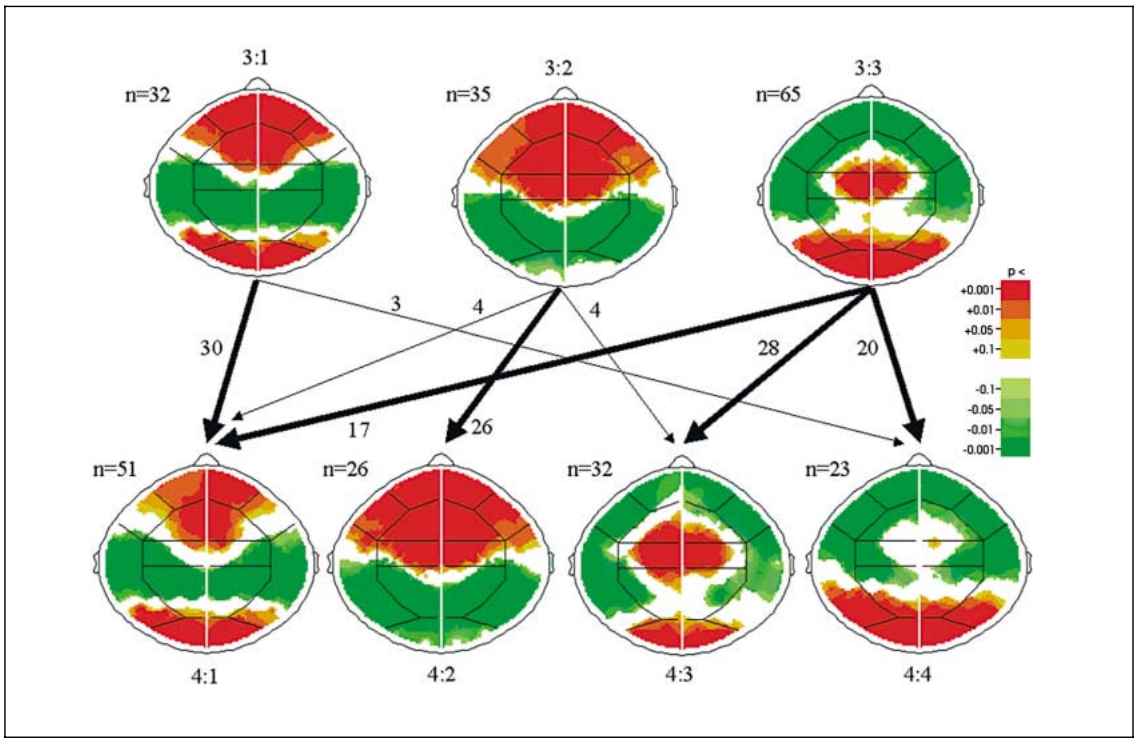

Fig. 4. The results of 3- and 4-cluster analyses. Upper images 3:1–3:3 represent Alzheimer clusters identified by the 3-cluster analysis, whereas lower images 4:1–4:4 are the clusters identified by the 4-cluster analysis. The lines indicate the number of subjects and their repositioning between clusters (fat line denotes major repositioning of subjects). The images show the statistical parametric differences between Alzheimer patients and the normal controls (Student's t test for independent samples). Statistically significant deviation from normal is coded according to the bar to the right. Red color indicates significantly higher values and green indicates significantly lower values than normal.

Table 1. Patient characteristics

	n	Age	Sex, m/f	MMSE	CBF[a]
Normal subjects	92	39.1 (13.6)	56/36	–	45.9 (7.2)
AD patients	132	74.1 (6.8)	38/94	21.4 (5.5)	36.9 (5.5)
3-cluster analysis					
3:1	32	72.8 (7.8)	9/23	20.9 (5.8)	36.4 (5.5)
3:2	35	74.1 (6.7)	13/22	20.2 (4.5)	36.7 (5.5)
3:3	65	74.8 (6.4)	16/49	22.4 (5.7)	37.5 (5.6)
4-cluster analysis					
4:1	51	73.0 (7.6)	12/39	21.8 (5.6)	38.1 (6.1)
4:2	26	73.8 (6.7)	10/16	20.1 (4.6)	36.2 (5.9)
4:3	32	76.8 (5.8)	9/23	21.1 (5.2)	36.2 (4.9)
4:4	23	73.3 (5.9)	7/16	22.7 (6.4)	36.0 (3.9)

[a] Uncorrected values for $P_E \cdot CO_2$.

significant age difference between the clusters of AD patients. The distribution of male and females was clearly in favor of females in all groups. The mean MMSE scores ranged from 20 to 23 points, indicating that patients could be regarded as having mild-to-moderate severity of cognitive decline. The cerebral perfusion values were not different between the clusters, and were slightly/moderately decreased compared with normal values.

Figure 4 summarizes the results from the clustering analyses of the AD patients into subgroups, sharing similar flow pathology. The illustrations show the statistically significant rCBF differences between the AD patients identified in each cluster, compared with the normal reference group (between-cluster differences were highly significant, results not shown). As can be seen in the 3-cluster analysis (top row) a temporal, temporoparietal flow pathology was present in all clusters (i.e. 3:1, 3:2, and 3:3). On the other hand, the pattern of flow pathology differed between the clusters, with respect to frontal lobe and occipital involvement. This was especially evident in cluster 3:3, which included patients with a dominant frontal and temporal flow pathology and with less of a parietal flow pathology. Patients in group 3:2 differed mainly by having lower occipital flow values than the other groups. The distribution of patients among the clusters was such that patients with a combined temporal and parietal rCBF pathology (3:1 and 3:2) represent 50.8% of the total patient group, while the remaining patients (49.2%, 3:3) had a predominant frontal and temporal flow pathology. The clustering of patients into four clusters (fig. 4) mainly resulted in a split of the original cluster 3:3. This resulted in a reclassification of patients into two groups (4:3 and 4:4) with a similar frontal and frontotemporal flow pathology. The major regional flow differences between these two groups were seen in the motor cortex, where patients in 4:3 showed significantly higher values than those in 4:4, and in temporal areas, where patients in 4:3 showed a more pronounced deficit.

Discussion

Neural networks have been previously used for the classification of functional brain images obtained with PET [9, 10] and SPECT [11–15]. With these techniques, information has been obtained in a large number of volume elements in a three-dimensional array. The information obtained with these methods usually has to be processed so that a reasonable number of inputs to the neural networks is achieved. This is generally accomplished by selection of regions of interest corresponding to various cortical areas. The number of inputs in the cited studies varies from 4 to 120. In most studies, the input to the neural networks only represents part of the information available. The selection of regions of interest may be automatic, but often entails subjective decisions. Several studies have shown neural networks to categorize patients as well as or better than experts [9, 14] and better than more conventional statistical methods [9, 12, 14, 15]. The performance of the neural networks appears to be dependent on the resolution of the imaging system and on the number of inputs to the neural network [10], so that better discrimination between pa-

tients with AD and normal subjects can be obtained with higher resolution and a larger number of inputs.

This study is the first in which neural networks have been applied to brain perfusion images obtained with ^{133}Xe washout. With this technique, only information about blood flow in the cortex is obtained, as the low photon energy of ^{133}Xe precludes studies of deeper structures. The 64-detector array used in this study thus provides information about the blood flow in a large proportion of the cortex. We chose to use the information from all detectors as input to the neural network. This means that although the imaging resolution of our system is far below that of PET or SPECT systems, we in fact used a larger number of inputs to the neural network than nearly all previous studies. Furthermore, we used all information available, and therefore no reduction of data in specific regions of interest was involved. This study also represents by far the largest number of patients with AD that has been investigated with neural networks to date. The result obtained for the classification of patients with AD in our study is compatible with the best results obtained in the previous studies using other brain imaging methods. It thus appears that neural networks are useful for the classification of functional brain images in the diagnosis of AD irrespective of the imaging technique used.

The neural networks used in this study provided a weight factor for each input, i.e. each detector, for the classification of studies. This information reflects the regions of the brain most likely to discriminate between patients with AD and normal subjects. The most important detectors were found in the left parietal region. We also found a statistically significant dominance for the detectors over the left hemisphere. This is in general agreement with previous studies, which have found a predominance of the flow reduction in the left parietal region to be typical for AD [34–38]. The importance of the detectors over the motor areas and the occipital lobes was somewhat surprising. It need not, however, be blood flow in these regions per se which is important for the classification of the patients. The neural network uses information from all detectors simultaneously in the analysis. It may therefore be that a low flow in the temporoparietal regions in combination with preserved flow in the surrounding regions is important for the classification. In fact, this combination of flow patterns has previously been described in a PET study by Kippenhan et al. [10], where the most important discriminatory profile of the neural network was a metabolic decrease in temporal and parietal areas in combination with higher normalized values in the motor-sensory and occipital regions.

AD is well defined from a histopathological point of view. It is well known that there is considerable heterogeneity among patients with AD clinically as well as with regard to functional imaging [10, 18]. In functional imaging studies, heterogeneity has often been noted but only rarely systematically analyzed. Holman et al. [18] studied rCBF in consecutive patients with memory loss or cognitive abnormalities. The SPECT images were classified into seven patterns by visual assessment. Among patients who subsequently developed AD, the characteristic pattern of bilateral temporal or parietal cortical defects was seen in 27% of cases. A further 38% of patients who developed AD had bilateral temporal or parietal defects plus additional defects. Fifteen percent of the patients had unilateral temporal or parietal defects, and 6% had frontal defects only. A large variation in functional brain deficits in AD has also been reported in several other SPECT studies [19, 20].

This study is, to the best of our knowledge, the first to use objective means for a systematic analysis of the heterogeneity in rCBF imaging in AD. In the analysis, each patient was placed in a multidimensional space, and patients showing similarities in the distribution of rCBF were categorized in clusters. These cluster analyses clearly demonstrated the existence of different patterns of rCBF pathology in patients with AD. In all clusters, there was reduced flow in the temporoparietal regions, and the clusters differed by the involvement of other regions, especially the occipital and the frontal regions. Reduced blood flow and glucose uptake in the frontal lobes have been noted in patients with AD previously [18, 34, 39]. A correlation between the extent of perfusion abnormalities and clinical severity of dementia has been described in several cross-sectional studies of patients with AD [34, 35, 40]. In this study, we did not find any significant differences between the rCBF clusters with age or with severity of dementia as assessed by the MMSE. Further studies are thus required to elucidate if the difference in the distribution of rCBF pathology is reflected in clinical characteristics of the patients or in the evolution of the disease.

Acknowledgments

This study was supported by grants from the Swedish Medical Research Council (9893), the Alzheimer Foundation and the Gamla Tjänarinnor Foundation.

References

1 Hofman A, Rocca WA, Brayne C, Breteler MM, Clarke M, Cooper B, Copeland JR, Dartigues JF, da Silva-Droux A, Hagnell O, et al: The prevalence of dementia in Europe: A collaborative study of 1980–1990 findings. Eurodem Prevalence Research Group. Int J Epidemiol 1991;20:736–748.

2 Braak H, Braak E: Neuropathological stageing of Alzheimer-related changes. Acta Neuropathol 1991;82:239–259.

3 Ingvar DH, Risberg J, Schwartz MS: Evidence of subnormal function of association cortex in presenile dementia. Neurology 1975;25:964–974.

4 Risberg J: Regional cerebral blood flow measurements by 133-Xe inhalation: Methodology and applications in neuropsychology and psychiatry. Brain Lang 1980;9:9–34.

5 Risberg J, Gustafson L: Regional cerebral blood flow measurements in the clinical evaluation of dementia patients. Dement Geriatr Cogn Disord 1997;8:92–97.

6 Warkentin S, Passant U, Brun A, Risberg J, Gustafson L: Cerebral blood flow in dementia related to neuropathological findings. Neurobiol Aging 1992;13(suppl 1):96.

7 Jobst KA: (OPTIMA) Alzheimer's disease is accurately diagnosed by combining Tc-99m HMPAO SPECT and temporal lobe oriented X-ray CT scans. J Nucl Med 1994;35:20P.

8 Davis PC, Gray L, Albert M, Wilkinson W, Hughes J, Heyman A, Gado M, Kumar AJ, Destian S, Lee C, et al: The Consortium to Establish a Registry for Alzheimer's Disease (CERAD). III. Reliability of a standardized MRI evaluation of Alzheimer's disease. Neurology 1992;42:1676–1680.

9 Kippenhan JS, Barker WW, Pascal S, Nagel J, Duara R: Evaluation of a neural-network classifier for PET scans of normal and Alzheimer's disease subjects. J Nucl Med 1992;33:1459–1467.

10 Kippenhan JS, Barker WW, Nagel J, Grady C, Duara R: Neural-network classification of normal and Alzheimer's disease subjects using high-resolution and low-resolution PET cameras. J Nucl Med 1994;35:7–15.

11 Chan KH, Johnson KA, Becker A, Satlin A, Mendelson J, Garada B, Holman BL: A neural network classifier for cerebral perfusion imaging. J Nucl Med 1994;35:771–774.

12 Dawson MRW, Dobbs A, Hooper HR, McEwan AJB, Triscott J, Cooney J: Artificial neural networks that use single-photon emission tomography to identify patients with probable Alzheimer's disease. Eur J Nucl Med 1994;21:1303–1311.

13 DeFigueiredo RJP, Shankle WR, Maccato A, Dick MB, Mundkur P, Mena I, Cotman CW: Neural-network-based classification of cognitively normal, demented, Alzheimer's disease and vascular dementia from single photon emission tomography image data from brain. Proc Natl Acad Sci USA 1995;92:5530–5534.

14 Page MPA, Howard RJ, O'Brien JT, Buxton-Thomas MS, Pickering AD: Use of neural networks in brain SPECT to diagnose Alzheimer's disease. J Nucl Med 1996;37:195–200.

15 Hamilton D, O'Mahony D, Coffey J, Murphy J, O'Hare N, Freyne P, Walsh B, Coakley D: Classification of mild Alzheimer's disease by artificial neural network analysis of SPECT data. Nucl Med Commun 1997;18:805–810.

16 Masterman DL, Mendez MF, Fairbanks LA, Cummings JL: Sensitivity, specificity, and positive predictive value of technetium 99-HmPAO SPECT in discriminating Alzheimer's disease from other dementias. J Geriatr Psychiatry Neurol 1997;10:15–21.

17 Claus JJ, van Harskamp F, Breteler B, Krenning EP, de Koning I, van der Cammen TJM, Hofman A, Hasan D: The diagnostic value of SPECT with TC 99m HMPAO in Alzheimer's disease: A population-based study. Neurology 1994;44:454–461.

18 Holman BL, Johnson KA, Gerada B, Carvalho PA, Satlin A: The scintigraphic appearance of Alzheimer's disease: A prospective study using technetium-99m-HMPAO SPECT. J Nucl Med 1992;33:181–185.

19 Waldemar G, Hoegh P, Paulson OB: Functional brain imaging with single-photon emission computed tomography in the diagnosis of Alzheimer's disease. Int Psychogeriatr 1997;9:223–227.

20 Zimmer R, Leucht S, Rädler T, Schmauss F, Gebhardt U, Lauter H: Variability of cerebral blood flow deficits in ^{99m}Tc-HMPAO SPECT in patients with Alzheimer's disease. J Neural Transm 1997;104:689–701.

21 McKhann G, Drachman D, Folstein M, Katzman R, Price D, Stadlan EM: Clinical diagnosis of Alzheimer's disease: Report of the NINCDS-ADRDA Work group under the auspices of Department of Health and Human Services Task Force on Alzheimer's disease. Neurology 1984;4:939–944.

22 Folstein MF, Folstein SE, McHugh PR: 'Mini-mental state'. A practical method for grading the cognitive state of patients for the clinician. J Psychiatr Res 1975;12:189–198.

23 Obrist WD, Thompson HK, Wang HS, Wilkinson WE: Regional cerebral blood flow estimated by 133-Xe inhalation. Stroke 1975;6:245–256.

24 Risberg J, Ali Z, Wilson EM, Wills EL, Halsey JH: Regional cerebral blood flow by 133-Xe inhalation: Preliminary evaluation of an initial slope index in patients with unstable flow compartments. Stroke 1975;6:142–148.

25 Cross SS, Harrison RF, Kennedy RL: Introduction to neural networks. Lancet 1995;346:1075–1079.

26 Rögnvaldsson T: On Langevin updating in multilayer Perceptrons. Neural Comput 1994;6:916–926.

27 Hanson SJ, Pratt LY: Comparing biases for minimal network construction with back-propagation; in Touretzky DS (ed): Advances in Neural Information Processing Systems. San Meteo, Kaufmann, 1989, pp 177–185.

28 Wehrens R, Putter H, Buydens LMC: The bootstrap: A tutorial. Chemom Intell Lab Syst 2000;54:35–42.

29 Bishop CM: Neural Networks for Pattern Recognition. Oxford, Oxford University Press, 1995, pp 187–189.

30 Davies DL, Bouldin DW: A cluster separation measure. IEEE Trans Pattern Anal Machine Intell 1979;1:224–227.

31 Rodriguez G, Warkentin S, Risberg J, Rosadini G: Sex differences in regional cerebral blood flow. J Cereb Blood Flow Metab 1988;8:783–789.

32 Hagstadius S, Risberg J: Regional cerebral blood flow characteristics and variations in resting normal subjects. Brain Cogn 1989;10:28–43.

33 Warkentin S, Passant U: Functional activation of the frontal lobes. Regional cerebral blood flow findings in normals and in patients with frontal lobe dementia performing a word fluency test. Dementia 1993;4:188–191.

34 Johnson KA, Kijewski MF, Becker JA, Garada B, Satlin A, Holman BL: Quantitative brain SPECT in Alzheimer's disease and normal aging. J Nucl Med 1993;34:2044–2048.

35 Keilp JG, Alexander GE, Stern Y, Prohovnik I: Inferior parietal perfusion, lateralization, and neuropsychological dysfunction in Alzheimer's disease. Brain Cogn 1996;32:365–383.

36 Sachdev P, Gaur R, Brodaty H, Walker A, Meares S, Koder D, Haindl W: Longitudinal study of cerebral blood flow in Alzheimer's disease using single photon emission tomography. Psychiatry Res 1997;68:133–141.

37 Mattmann A, Feldman H, Forster B, Li D, Szasz I, Beattie BL, Schulzer M: Regional HmPAO SPECT and CT measurements in the diagnosis of Alzheimer's disease. Can J Neurol Sci 1997;24:22–28.

38 Celsis P, Agniel A, Cardebat D, Démonet JF, Ousset PJ, Puel M: Age related cognitive decline: A clinical entity? A longitudinal study of cerebral blood flow and memory performance. J Neurol Neurosurg Psychiatry 1997;62:601–608.

39 Piert M, Koeppe RA, Giordani B, Berent S, Kuhl DE: Diminished glucose transport and phosphorylation in Alzheimer's disease determined by dynamic FDG-PET. J Nucl Med 1996;37:201–208.

40 Jagust WJ, Haan MN, Eberling JL, Wolfe N, Reed BR: Functional imaging predicts cognitive decline in Alzheimer's disease. J Neuroimaging 1996;6:156–160.